Design study of Low Loss Single-Mode Hollow Core Photonic Crystal Terahertz Waveguide with Support Bridges

Binbin Hong, Nutapong Somjit, John Cunningham, and Ian Robertson
School of Electronic and Electrical Engineering, University of Leeds, Leeds, LS2 9JT UK

***Abstract*— We present a design study of an all-polymer low loss single-mode hollow-core photonic crystal (HCPC) terahertz (THz) waveguide with dielectric bridges used as mechanical supports. By exploiting a modal-filtering effect and Brewster phenomenon, we maximize the loss discrimination between the fundamental and other higher order modes resulting in an effectively single-mode operation, though the HCPC THz waveguide is ostensibly multi-mode. Owing to the use of support bridges, which increase the propagation loss, the non-ideal HCPC THz waveguide has higher loss than an ideal one. Nonetheless, the propagation loss of the fundamental HE_{11} mode can still be minimized, to lower than 5 dB/m over the frequency range from 0.75 to 1.1 THz. In addition, the group velocity dispersion of the HE_{11} mode is less than -0.5 ps/THz/cm.**

I. INTRODUCTION

THE strong demand for compact and robust THz systems provides a strong motivation for the study of terahertz waveguides. However, due to the high losses in both metals and dielectric materials in the THz frequency regime, the realization of low loss single-mode THz waveguide has proved challenging. Since the lowest absorption loss occurs for dry air, it is essential in a THz waveguide to maximize the fraction of power guided by air-gaps. Due to their photonic bandgap, air core HCPCs are able to confine THz waves in their (hollow) core region, thus reducing overall loss.

II. RESULTS

The HCPC THz waveguide studied consists of an air core ($n_c = 1$) surrounded by periodic multilayer dielectric cladding (concentric layers) of alternately high (n_a) and low (n_b) refractive index materials, the thickness of which are a and b respectively, while the core radius is r_c. In addition, a perfectly matched layer (PML) is applied at the outermost layer during the calculation, performing as an perfectly absorbing layer with thickness and refractive index of 2Λ ($\Lambda = a + b$) and n_a, respectively. By using a modified half-wavelength condition, which associates the material and geometry parameters with the bandwidth, one can easily manipulate the bandgap shape [1].

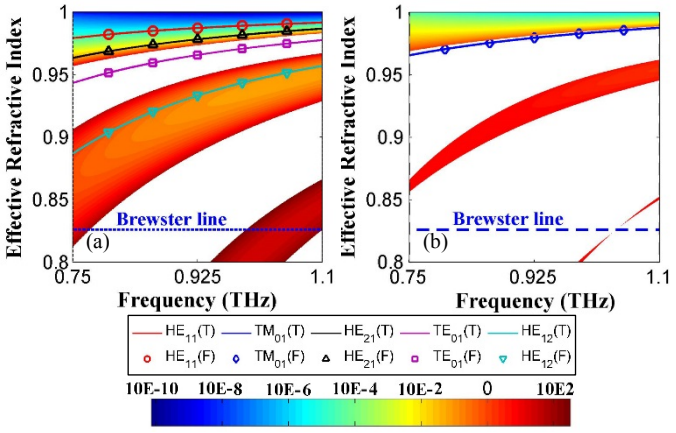

Fig. 1. Bandgap, confinement loss diagram and dispersion curves of the TE/HE modes (a) and the TM/EH modes (b). The colored region represents the band-stop region and the confinement loss (unit: dB/m) of the waveguide simultaneously. Here, $n_a = 1.4649 + 0.00041i$, $n_b = 1$, a=92 μm, b=570 μm, r_c=745 μm, and the period number is 5. T and F in the legend represent the results calculated by the theoretically transfer matrix method and the numerically finite element method, respectively. The effective refractive index at the Brewster angle is 0.826.

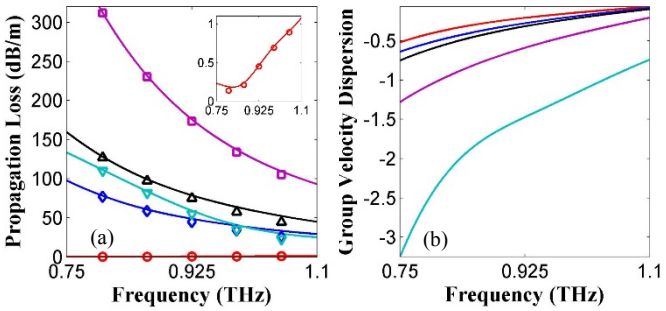

Fig. 2. (a) Propagation loss and (b) group velocity dispersion (unit: ps/THz/cm). The legend is the same as that of Fig. 1.

After comparing several low loss polymers, TPX (Polymethylpentene) was chosen as the high refractive index material for its relatively lower loss, and air is chosen as the low refractive index material, so that Brewster phenomenon could be used to filter out undesirable TM modes [2]. The measured frequency-dependent complex refractive index of TPX is used to calculate the dispersion and loss, but only the mean value of approximately $1.4649 + 0.00041\mathrm{i}$ is used to calculate the bandgap since its slight changes over the frequency range of interest have negligible effects on the bandgap shape.

The bandgap and the confinement loss diagram [2] are shown in Fig. 1 simultaneously, as well as the dispersion curves of five representative modes. The cladding period is set to five because above this value the propagation loss for the main HE_{11} mode does not change significantly. The theoretical results calculated by the transfer matrix method compare well with the numerical simulation results calculated by the finite element method using COMSOL. The colored region in Fig. 1 illustrates the band-stop region and the confinement loss of the HCPC THz waveguide. The confinement loss, which takes into account only the loss due to the scattering of the multilayer cladding rather than the material absorption, is represented by different colors, with the loss decreasing from red to blue. Owing to the finite number of the cladding layers, the guiding modes in the band-stop are intrinsically leaky since the confinement is not perfect, and their power decay rates in the periodic claddings are associated with their confinement loss. The lower the confinement loss is, the higher the power decay rate will be, and the better the mode is confined. From Fig. 1, the confinement loss at the edge of the bandgap is higher than that in the center region of the same order bandgap; and the confinement loss in the lower order bandgap is generally lower

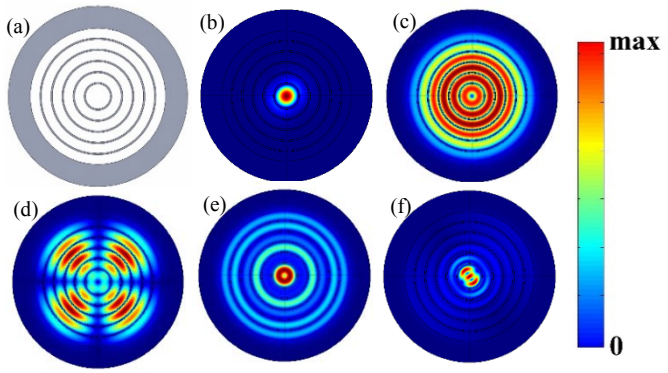

Fig. 3. (a) Geometry of the ideal HCPC THz waveguide without support bridges. (b) – (f) are the normalized electric fields of HE_{11}, TM_{01}, HE_{21}, TE_{01} and HE_{12} at 1.1 THz, respectively.

than that in the higher order bandgap over the same frequency range, except that the confinement loss at the edge of the lower order bandgap may be higher than that in the center region of the higher order bandgap; we also note that wider bandgaps generally have lower confinement losses in HCPC structures [1]. In addition, due to the Brewster phenomenon, the bandgaps for TM/EH modes are much narrower than that for TE/HE modes since they always close up completely at all effective refractive indexes which lie on the Brewster line, as shown by the third order bandgap (Fig. 1 (b)). This behavior sees the TM_{01} mode, the lowest order TM/EH mode, lying outside the band-stop region, and helps to increase the confinement loss of other higher order TM/EH modes over the same frequency range. Therefore, a substantial loss discrimination between the fundamental HE_{11} mode and all other higher order modes can be achieved.

The propagation loss of the five modes are presented in Fig. 2 (a), including scattering losses and material absorption. The propagation loss of the fundamental HE_{11} mode (<1.1 dB/m) is much lower than the other higher order modes (>22 dB/m) over the frequency range from 0.75 to 1.1 THz. Correspondingly, in Fig. 3, the fundamental HE_{11} mode has maximum confinement within the air core, while other modes are leaky and will

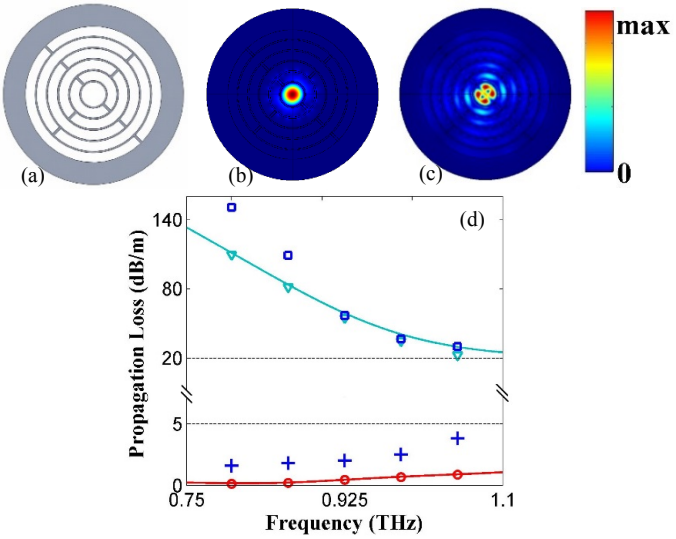

Fig. 4. (a) Geometry of the nonideal HCPC THz waveguide with designed support bridges. (b) and (c) are the normalized electric fields of HE_{11} and HE_{12} at 0.925 THz, respectively. (d) The propagation losses of HE_{11} and HE_{12} in nonideal HCPC THz waveguide. The legend is the same as that of Fig. 1, except for the blue cross and the blue square which represents the propagation loss of HE_{11} and HE_{12}, respectively.

experience essentially the high attenuation of the bulk cladding materials. This loss-induced modal discrimination creates a modal-filtering effect [4] resulting in an effectively single-mode operation in the HCPC THz waveguide which is ostensibly multi-mode. In addition, the group velocity dispersion of HCPC THz waveguide is very small, as shown in Fig. 2 (b). The theoretical group velocity dispersion of the fundamental HE_{11} mode is less than -0.5 ps/THz/cm.

A HCPC THz waveguide which use air as one of its cladding materials naturally requires mechanically support bridges to maintain the air gaps between the claddings. The effects of the dielectric bridges on the propagation losses and the mode structure are illustrated in Fig. 4. Attributing to the small air core and less cladding periods, it is possible to maintain the air gaps with only a few bridges. The optimized design of the HCPC THz waveguide with support bridges is shown in Fig. 4(a). The width of the support bridges is designed to 112 μm, which is optimized for minimum propagation loss of the fundamental HE_{11} mode. As the mode structures of TM_{01}, HE_{21} and TE_{01} are very leaky, this results in weak competition with the fundamental HE_{11} mode. Thus, we selected HE_{11} mode and the HE_{12} mode for comparison. Comparing Fig. 3 (b) to Fig. 4 (b), we can see that the electric field vanishes at the interface of the core and the first cladding; the HE_{11} mode is tightly confined within the air core and is less affected by the disturbance from the environment. However, due to the looser confinement, the mode structure of the HE_{12} mode is affected by the asymmetric bridges, as shown in Fig. 4 (c). Overall, the support bridges slightly increase the losses of the HE_{11} mode and the HE_{12} mode. Nonetheless, the propagation loss of the main HE_{11} mode can still be minimized to lower than 5 dB/m, while that of the HE_{12} mode is larger than 23 dB/m. The substantial loss discrimination between the main HE_{11} mode and its competition modes ensure that the HCPC THz waveguide operates effectively in single-mode fashion.

III. Summary

We reported a novel low loss single-mode Bragg fiber with support bridges. The propagation loss and the group velocity dispersion of the fiber are less than 5 dB/m and -0.5 ps/THz/cm, respectively. The propagation loss of the main HE11 mode is lower than 5 dB/m, while that of its main competition mode (HE12) is higher than 23 dB/m. The loss-induced modal discrimination results in an effectively single-mode operation, though the HCPC THz waveguide is ostensibly multi-mode. All of these advantages make the HCPC THz waveguide a strong candidate for compact and robust THz system.

BBH wishes to acknowledge Y. Zhang, M. Swithenbank, and N. Greenall for their helpful discussions.

References

[1]. B. Hong, et al. "Hollow core photonic crystal for terahertz gyrotron oscillator," *J. Phys. D: Appl. Phys.*, vol. 48, pp. 045104, January, 2015.
[2]. Y. Zhang, & I. D. Robertson, "Analysis and design of Bragg fibers using a novel confinement loss diagram approach," *Lightwave Technology, Journal of*, vol. 28, pp. 3197-3206. November, 2010.
[3]. P. Yeh, A. Yariv, & E. Marom, "Theory of Bragg fiber," *JOSA*, vol. 68, pp. 1196-1201, September, 1978.
[4]. M. Ibanescu, et al. "Analysis of mode structure in hollow dielectric waveguide fibers," *Physical review E*, vol. 67, pp. 046608, April, 2003.